ERIS adaptive optics system design

Enrico Marchetti*[a], Miska Le Louarn[a], Christian Soenke[a], Enrico Fedrigo[a],
Pierre-Yves Madec[a], Norbert Hubin[a]
[a]European Organization for Astronomical Research in the Southern Hemisphere,
Karl-Schwarzschild-Str. 2, D-85748 Garching bei München, Germany

ABSTRACT

The Enhanced Resolution Imager and Spectrograph (ERIS) is the next-generation instrument planned for the Very Large Telescope (VLT) and the Adaptive Optics facility (AOF). It is an AO assisted instrument that will make use of the Deformable Secondary Mirror and the new Laser Guide Star Facility (4LGSF), and it is planned for the Cassegrain focus of the telescope UT4. The project is currently in its Phase A awaiting for approval to continue to the next phases.

The Adaptive Optics system of ERIS will include two wavefront sensors (WFS) to maximize the coverage of the proposed sciences cases. The first is a high order 40x40 Pyramid WFS (PWFS) for on axis Natural Guide Star (NGS) observations. The second is a high order 40x40 Shack-Hartmann WFS for single Laser Guide Stars (LGS) observations. The PWFS, with appropriate sub-aperture binning, will serve also as low order NGS WFS in support to the LGS mode with a field of view patrolling capability of 2 arcmin diameter. Both WFSs will be equipped with the very low read-out noise CCD220 based camera developed for the AOF. The real-time reconstruction and control is provided by a SPARTA real-time platform adapted to support both WFS modes.

In this paper we will present the ERIS AO system in all its main aspects: opto-mechanical design, real-time computer design, control and calibrations strategy. Particular emphasis will be given to the system performance obtained via dedicated numerical simulations.

Keywords: Adaptive Optics, Laser Guide Stars, Pyramid Wavefront Sensor, Deformable Secondary Mirror

1. INTRODUCTION

ERIS[1] is the new IR instrument for the Adaptive Optics Facility[2] (AOF) to be installed at the Cassegrain focus of VLT's UT4. It consists of an AO module comprising the wave front sensors (WFS) and the Real-Time Computer (RTC), feeding SPIFFI, the Integral Field Unit spectrograph currently included in the SINFONI[3] instrument, and a new near-infrared imaging camera that is supposed to take over some of the most used observing modes of NACO[4].

ERIS performs high spatial resolution spectroscopic and imaging observations at infrared (IR) wavelengths enabled by high Strehl AO correction on a narrow Field of View (FoV).

ERIS uses and depends on the AOF infrastructure to perform the narrow FoV AO correction and its implementation maximizes the re-use of existing sub-systems and components developed in the framework of the AOF. In particular, the AO correction is provided by the AOF Deformable Secondary Mirror (DSM) and the artificial Laser Guide Stars (LGSs) are generated by the Four Laser Guide Star Facility (4LGSF) system. Natural Guide Stars (NGS) are also used for specific observations.

In this paper we present the design of the ERIS AO system (hereafter refereed as ERIS AO module). Starting from the AO module requirements the AO module performance obtained via dedicated numerical simulations will be described. Then the opto-mechanical design, the real-time computer design, the control and the calibrations strategy will be outlined.

*emarchet@eso.org; phone +49 89 32006458; fax +49 89 3202362

2. AO MODULE REQUIREMENTS

The design of ERIS AO module is done according to the ERIS Top-Level Requirements (TLRs). The TLRs most relevant for the AO design are the following:

- The instrument shall be mounted at UT4 Cassegrain.
- The instrument will use the DSM and, at least, one of the AOF lasers.
- The Strehl ratio at 2.2 μm under standard atmospheric conditions (0.87 arcsec seeing) shall be:
    - For NGS wavefront sensing≥80% in the direction of the NGS (on-axis) for an m_R=8 star. Off-axis performance follows anisoplanatism.
    - For LGS wavefront sensing≥65% in the direction of the LGS (on -axis) for an m_R=12 on-axis low order correction NGS. On-axis performance with off-axis low order correction NGS follows atmospheric tip-tilt anisoplanatism.
- The (above) Strehl ratios shall not be degraded due to instrumental reasons by more than 5% (absolute) during observations of 15min.
- For the LGS wavefront sensing the Strehl ratio for a low order correction NGS down to m_R=17 shall be not less than half of the Strehl ratio obtained with a m_R=12 low order correction NGS at the same the off-axis distance.
- For the LGS wavefront sensing the search field for the low order correction NGS shall allow to find an $m_R \leq 17$ star in 30% of the pointings at the Galactic pole. The associated Strehl ratio performance will depend on the atmospheric tip-tilt anisoplanatism and on the tip-tilt star magnitude.

The derived guidelines for the AO module design can be summarized as following:

- The AO module is designed to be accommodated at the UT4 **Cassegrain** and to minimize the impact of instrumental perturbations (for example flexures) on the correction performance.
- The AO module makes use of the AOF's **DSM** (1170 actuators) for correcting the on-axis atmospheric turbulence.
- The AO module makes use of at least **one laser and launch telescope of the 4LGSF** to generate the LGS wavefront sensing source.
- The AO module is equipped with **one high order NGS wavefront sensor** for on-axis atmospheric turbulence correction. The number of sub-apertures should be dimensioned in order to fully exploit the DSM correction capabilities guaranteeing high Strehl ratio performance.
- The AO module is equipped with **one high order LGS wavefront sensor** for on-axis atmospheric turbulence correction. The number of sub-apertures and the FoV should be dimensioned in order to fully exploit the DSM correction capabilities and to cope with the LGS post elongation to guarantee high Strehl ratio performance.
- The AO module is equipped with **one low order NGS wavefront sensor** supporting the LGS wavefront sensor to compensate for tip-tilt indetermination due to the LGS use. The number of sub-apertures should be dimensioned to guarantee both the most precise low order correction and the accessibility to the faintest wavefront sensing sources. The NGS searching FoV is dimensioned to achieve the required sky coverage.

After a careful trade off phase the following system main characteristics have been set:

- High Order **NGS WFS: the Pyramid WFS (PWFS)**, 40×40 sub-apertures.
- High Order **LGS WFS: the Shack-Hartmann WFS (SHWFS)**, 40×40 sub-apertures (identical copy of the WFSs used for the AOF).
- Low Order **NGS WFS: the Pyramid WFS** 2×2 sub-apertures (it is the high order NGS WFS used in a different configuration).

In order to maximize re-using of existing sub-systems and components developed in the framework of the AOF, the following key components have been identified for the design of the AO module:

- **WFS CCD cameras: CCD220** used as standard detector for the AOF LGS WFSs and visible NGS low order sensors;
- **WFS CCD camera controllers**: ESO's standard **New General detector Controller (NGC)** used by AOF and by all future ESO instruments;
- **Real-Time Computer: SPARTA**[5] platform used by AOF. SPARTA functionalities and features can be massively re-used for the AO module implementation.

3. ADAPTIVE OPTICS PERFORMANCE

In order to evaluate the ERIS AO module correction performance and sensitivity to main input parameters a complete set of numerical simulations have been performed with the ESO AO simulations tools OCTOPUS[6]. The simulations constitute the end-to-end modeling of all the steps involving the AO system main functionality and the input disturbance generation and propagation. The input parameters are the following:

Deformable Secondary Mirror configuration

- AOF DSM real geometry, 1170 actuators

High Order NGS WFS configuration

- Pyramid WFS, 40×40/20×20/10×10 sub-ap, 2.5 arcsec FoV diameter
- Central sensing wavelength: 0.7 μm

High Order LGS WFS configuration

- Shack-Hartmann, 40×40 sub-ap, 6×6 px/sub-ap, 0.83 arcsec/px
- Central sensing wavelength: 0.589 μm

Low Order NGS WFS configuration

- Pyramid, 2×2 sub-ap, 2.5 arcsec FoV diameter
- Central sensing wavelength: 0.7 μm

WFS detector characteristics (from CCD220)

- RON (Read-Out Noise): 1.0 e^-/px/frame (or e^-/binned pixel/frame)
- Dark: 1.2 e^-/px/s (including the Clock-Induced Charge)
- Excess noise: $\sqrt{2}$
- Charge diffusion: FWHM 0.55 px

LGS related characteristics

- LGS launch location: Δx=1250 mm, Δy=5350 mm (with respect to the pupil/M1 center)
- LGS flux: 8×10^4 detected photons/s/sub-ap (without considering the excess noise)
- LGS spot size: 1.3 arcsec FWHM (small axis), short exposure
- LGS spot residual jitter: 120 mas rms, random Gaussian (quadratic sum of two orthogonal axes)
- Sodium profile: Gaussian, 10 km FWHM

Control loop characteristics

- High order WFS (NGS and LGS) reconstruction modal basis: Karhunen-Loeve
- High (NGS and LGS) and Low order WFS (NGS) loop maximum frequency: 1.2 kHz
- High (NGS and LGS) and Low order WFS (NGS) control loop delay: 1 to 3 depending on loop frequency
- Loop controller: simple integrator
- Shack-Hartmann centroiding algorithm: weighted centroid of gravity

Telescope pupil

- Diameter: 8m
- Central obstruction: 0.14 (linear ratio)

Sky background

- Sky background: 3300 detected photons/s/VLT-pupil/arcsec^2 (m_R=20.5/arcsec^2, 7 days Moon)

Atmospheric conditions

The atmospheric conditions used for the simulations are: seeing 0.87 arcsec (at 500nm, 30 degrees off Zenith), labeled as "DIMM seeing 0.8 arcsec".

- Fried parameter (r_0): 0.119 m
- Outer Scale (L_0): 22 m
- Coherence time (τ_0): 3.0 ms

The atmosphere is made of 10 layers (see Table 1):

Table 1. Atmospheric model sued for the ERIS AO module simulations

Layer number	**1**	**2**	**3**	**4**	**5**	**6**	**7**	**8**	**9**	**10**
Height (m)	1.16*30	1.16*140	1.16*281	1.16*562	1.16*1125	1.16*2250	1.16*4500	1.16*7750	1.16*11000	1.16*14000
C_n^2 fraction	0.59	0.02	0.04	0.06	0.01	0.05	0.09	0.04	0.05	0.05
Speed (m/s)	6.6	5.9	5.1	4.5	5.1	8.3	16.3	30.2	34.3	17.5

Other seeing values have been used in the simulations for the extended performance evaluation. They are labeled "DIMM seeing 0.6-1.0-1.2 arcsec".

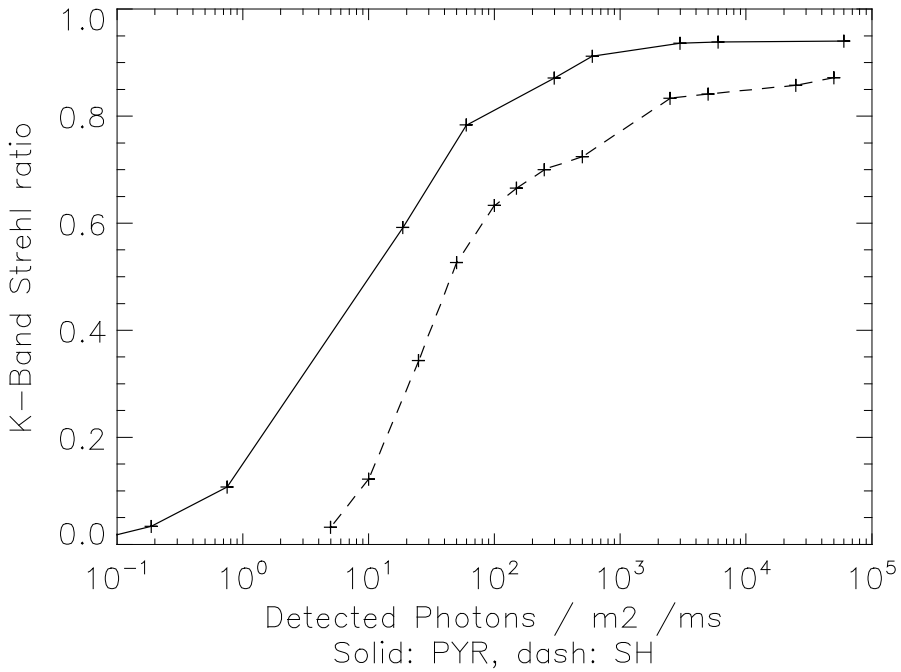

Figure 1. High order NGS PWFS correction performance (solid line): K band on-axis Strehl vs.NGS flux. As comparison the SHWFS performance (same configuration) is shown (dashed line). Error budget is not included.

The high order NGS PWFS on-axis performance vs. NGS flux (error budget not included) is shown in Figure 1. The level of correction is significantly higher than the one obtained with the SHWFS in the same configuration (dashed line). The following flux-magnitude conversion has been computed (see Table 2):

Table 2. Flux-R magnitude conversion for the NGS WFS

Flux [ph/m^2/ms]	0.1	1	10	100	1000
R magnitude (G0V)	20.0	17.5	15.0	12.5	10.0

The maximum K Band on-axis Strehl is ~0.94 (m_R< 9) It is worth noting that a non negligible value of 0.2 K Band on-axis Strehl is obtained for a magnitude m_R~16.5.

The high order LGS SHWFS on-axis performance vs. low order NGS off axis position (error budget not included) for different DIMM seeing values is shown in Figure 2. For the nominal "DIMM seeing 0.8 arcsec" the K band Strehl is 0.71 when the low order NGS is on axis with the LGS and drops to 0.33 at 60 arcsec off-axis. The NGS is supposed to be infinitely bright (no photon noise). The sampling is 40×40 at bright flux down to 10×10 for the faintest flux. The maximum loop frequency is 1.2 kHz (bright flux) down to 300 Hz (faintest flux).

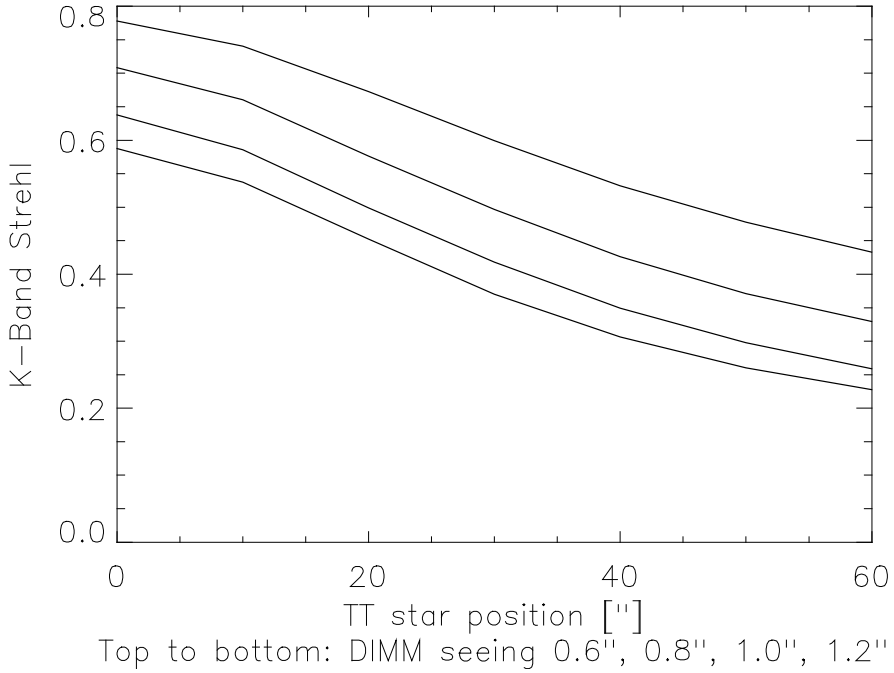

Figure 2. High order LGS SHWFS correction performance: K band on-axis Strehl vs.low order NGS off axis position. From top to bottom: DIM seeing 0.6, 0.8,1.0 and 1.2 arscec. The NGS is infinitely bright (no photon noise). Error budget is not included.

The high order LGS SHWFS on-axis performance vs. on-axis low order NGS flux (error budget not included) for different DIMM seeing values is shown in Figure 3. For the nominal "DIMM seeing 0.8 arcsec" the maximum K band Strehl holds up to m_R=14.5, drops to 0.60 for m_R=17.5, and still retains a non negligible values of 0.25 for mR=20.5. The loop frequency goes from 1.2 kHz for the brightest flux down to 120 Hz for the faintest point of the curves.

The sky coverage for the LGS mode at different Galactic latitudes is shown in Figure 4. The sky coverage computation is made taking into account the performance estimated in Figure 2 and Figure 3 and adding an error budget (143 nm rms WFE) which makes the final LGS performance matching the top level requirements.

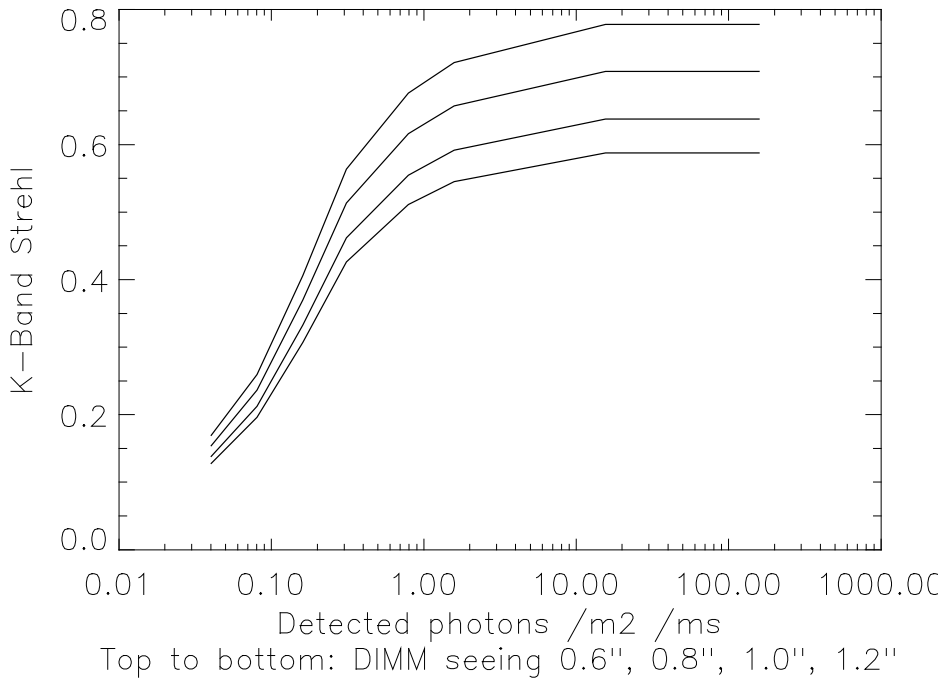

Figure 3. High order LGS SHWFS correction performance: K band on-axis Strehl vs. on-axis low order NGS flux. From top to bottom: DIM seeing 0.6, 0.8,1.0 and 1.2 arscec. Error budget is not included.

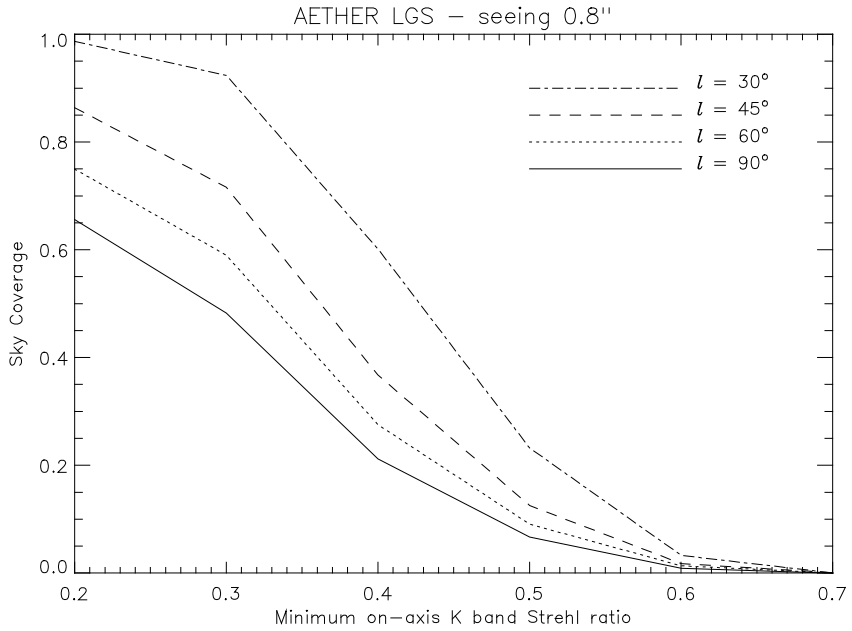

Figure 4. LGS mode sky coverage vs. on-axis Strehl for different galactic latitudes. Performance are for “DIMM seeing 0.8 arcsec”. Error budget matching the top level requirements has been included.

4. ADAPTIVE OPTICS DESIGN

The ERIS AO module is mounted on a bench located inside the ERIS supporting structure which is hosting the IR camera and providing an interface for the spectrograph SPIFFI (see Figure 5, left). The AO bench is supporting the dichroic separating the visible light (for the AO) and the IR light for the IR camera and SPIFFI), the NGS and the LGS WFSs and the calibration unit. A view of the AO bench is given in Figure 5, right.

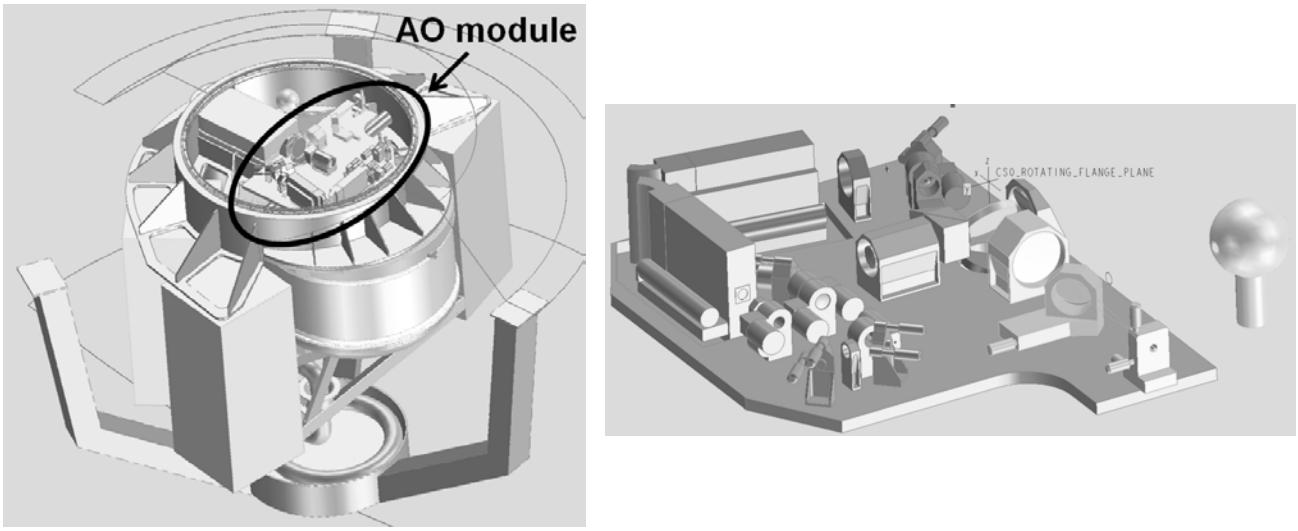

Figure 5. Left: ERIS subsystems assembly. The AO module (in the oval) is located on a bench inside the ERIS supporting structure. Right: ERIS AO module.

4.1 NGS WFS path

The 3D view of the NGS WFS path is show in Figure 6. The light coming from the telescope is separated by a dichroic reflecting the visible light (λ<1.0 μm) toward the AO module and transmitting the IR light (λ>1.0 μm) toward the science instruments. The visible light is then folded again to align the optical axis parallel to the telescope rotator plane. The transmitted FoV both to the AO module and to the science instruments is 2 arcmin diameter. A beam splitter cube, acting as notch filter, transmits the visible light toward the NGS WFS and reflects the light from the LGS (λ =0.589 μm, $\Delta\lambda$ ~15 nm TBC) toward the LGS WFS.

A pupil reimaging lens system re-images the telescope pupil (diameter 20.9 mm) on a field selector mirror. The field selector is able to bring any reference source in 2 arcmin diameter FoV at the center of the NGS WFS FoV (31% sky coverage at the Galactic pole). The field selector provides to re-acquire the NGS during observations when jittering (small and large offsets) is implemented. The field selector is also driven during observations to compensate for the image drift between visible (AO WFS) and IR (science instruments) wavelengths due to the differential atmospheric dispersion and for the instrument flexures. From the Field Selector on the transmitted FoV is 5 arcsec diameter.

An Atmospheric Dispersion Corrector (ADC) is located after the Field Selector. It includes also a re-imaging lens to create and intermediate focal plane. The ADC compensates for the reference source elongation due to the differential atmospheric dispersion. An optical derotator compensates for the rotation of the DSM's image on the NGS WFS. In fact the whole ERIS module is rotating to maintain fixed the orientation with respect to the sky. Consequently the image of the DSM rotates on the reference system of the AO module.

A pupil stabilization mirror is located at the intermediate F/9.7 focal plane created by the re-imaging lens coupled to the ADC. The scope of this function is to compensate for the DSM image shift on the NGS WFS. A re-imaging lens creates the final F/40.9 focal plane (1.59 mm/arcsec) in front of the NGS WFS and an intermediate pupil of 4.8 mm diameter where a Fast Jitter Mirror is located. The scope of the Fast Jitter Mirror is to continuously move the reference source image in front of the NGS WFS during closed loop operations, hereafter referred as "modulation". A wheel holding a set of FoV diaphragms and Neutral Density filters (not shown in Figure 6) assures narrowing the PWFS FoV and to dim the

incoming light in the case of bright NGS reference source. A notch filter provides to reject contamination from the remaining Sodium light leaking from the beam splitter cube. At the F/40.9 focal plane is located a refractive pyramid with four faces: this optical element splits the incoming light in four slightly diverging sub-beams. A lens assembly provide then to re-image the telescope pupil, one pupil per sub-beam, on the CCD220 detector.

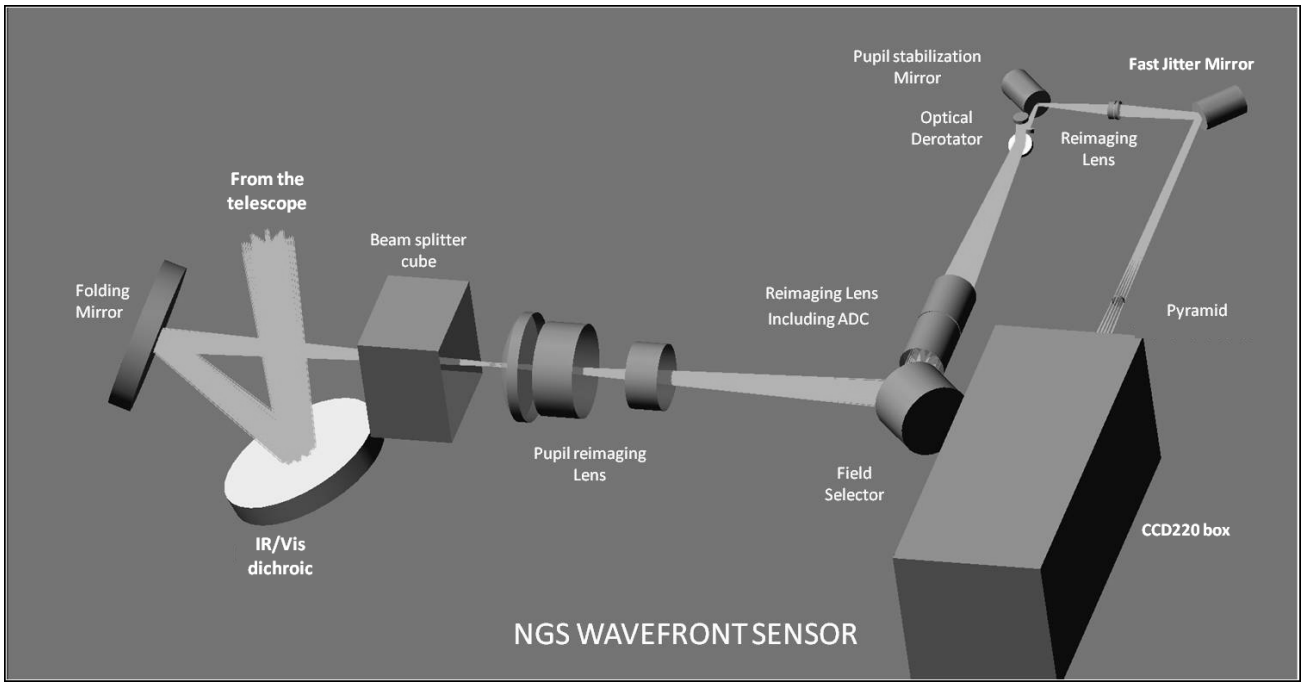

Figure 6. NGS WFS optical path.

4.2 High order WFS description

The High Order NGS WFS is the Pyramid WFS. The incoming light is split in four slightly diverging sub-beams by a refractive pyramid. A lens assembly re-images for each beam the telescope pupil (0.960 mm diameter) on the detector. The maximum transmitted FoV is 5 arcsec diameter. A filter wheel in front of the refractive pyramid is supporting different diaphragm to narrow the FoV (down to 1 arcsec TBC) and Neutral Density filters to dim the light of bright NGS reference sources in order stay within the linearity range of the detector (Neutral Density=1 largely enough for mR~0).

The pixels of the detector act as sub-apertures: each pupil is mapped by 40×40 pixels equivalent to 40×40 sub-apertures. The number of sub-apertures can be reduced down to 10×10 by binning the detector pixels before reading them out (4×4 binning).

For closed loop operations the image of the NGS reference source is modulated along a circular path around the tip of the refractive pyramid by means of the fast jitter mirror. The amplitude of the modulation is selected by the user according to seeing condition and NGS reference source magnitude. The speed of the modulation is locked to the detector integration time and synchronized by the detector controller: always one full modulation loop per integration time. The maximum detector frame rate is 1200 Hz.

The stabilization of the pupil image on the detector is guaranteed by the ancillary loop driving the Pupil stabilization mirror. The main characteristics of the High Oder PWFS are listed in Table 3.

Table 3. High order NGS WFS main parameters

Parameter	Value	Note
n. of pupils	4	-
FoV	5 arcsec diameter	-
n. of sub-apertures per pupil	40×40... 10×10	Binning 1×1...4×4
Pixels per sub-aperture per pupil	1×1	Binned pixel
Pupil size	0.960 mm	-
Detector	CCD220	-
Maximum frame rate	1200 Hz	-
Modulation type – amplitude	Circular – 0...10×λ/D	User defined
Modulation speed	= detector integration time	-

4.3 Low order NGS WFS description

All the functionalities of the Low Order NGS WFS are provided by the High Order PWFS, in fact the High Order PWFS works also as Low Order NGS. The only difference consists in the number of sub-apertures. In order to measure the tip-tilt and the focus the Low Order NGS WFS has 2×2 sub-apertures per pupil. The smaller number of sub-apertures is obtained by binning the pixels before reading them out (20×20 binning). The main characteristics of the low order NGS WFS are listed in Table 4.

Table 4. Low order NGS WFS main parameters

Parameter	Value	Note
n. of pupils	4	-
FoV	5 arcsec diameter	-
n. of sub-apertures per pupil	2×2	Binning 20×20
Pixels per sub-aperture per pupil	1×1	Binned pixel
Pupil size	0.960 mm	-
Detector	CCD220	-
Maximum frame rate	1200 Hz	-
Modulation type – amplitude	Circular – 0...10×λ/D	User defined
Modulation speed	= detector integration time	-

4.4 LGS WFS path

The 3D view of the LGS WFS path is shown in Figure 7. The light coming from the telescope is separated by a dichroic reflecting the visible light (λ<1.0 μm) toward the AO module and transmitting the IR light (λ>1.0 μm) toward the science instruments. The visible light is then folded again to align the optical axis parallel to the telescope rotator plane. The transmitted FoV is 5 arcsec diameter.

A beam splitter cube, acting as notch filter, reflects the light from the LGS (λ=0.589 μm, $\Delta\lambda$ ~15 nm TBC) toward the LGS WFS and transmits the visible light toward the NGS WFS.

An optical system provides compensates the variation of the LGS distance due to the telescope elevation angle (from 80 to 240 km). The focus compensator is also used to finely adjust the variations of the LGS mean altitude variations due to the change of the Sodium vertical profile structure. As for the NGS WFS, an optical derotator compensates for the rotation of the DSM's image on the LGS WFS.

A pupil stabilization mirror is located at the intermediate F/7.9 focal plane created by focus compensator. The scope of this function is to compensate for the DSM image shift on the LGS WFS. After the pupil stabilization mirror a collimator reimages a telescope pupil of 5.760 mm on a lenslet array with a focal length of 4.217 mm. The lenslet array is glued on the WFS camera window. The Shack-Hartmann spots are imaged directly on the CCD220 detector plane.

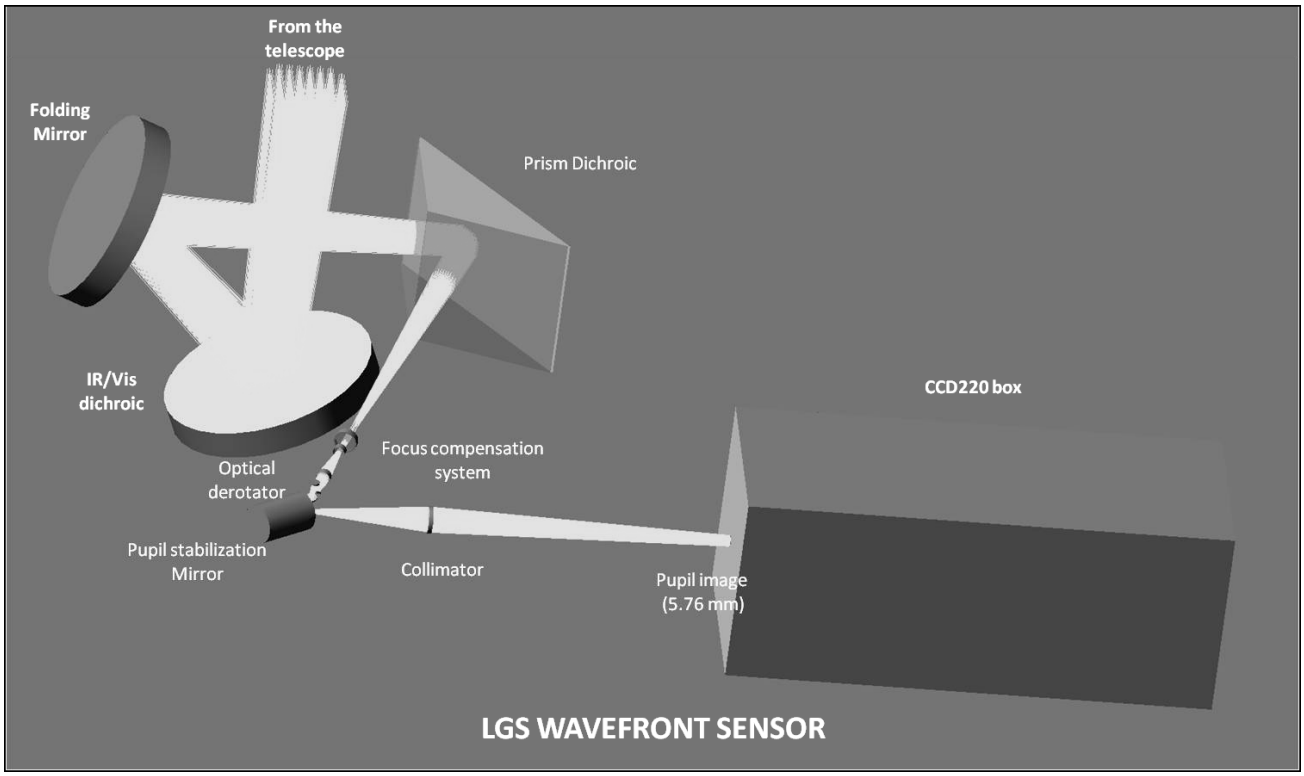

Figure 7. NGS WFS optical path.

4.5 High order LGS WFS description

The High Order LGS WFS is a Shack-Hartmann WFS identical copy of the AOF LGS WFSs. The transmitted FoV is 5 arcsec diameter. The number of sub-apertures is 40×40, 6×6 pixels each, so the full CCD220 detector area is used.The maximum detector frame rate is 1200 Hz.

The stabilization of the pupil image on the lenslet array is guaranteed by the ancillary loop driving the Pupil stabilization mirror. The main characteristics of the High Oder LGS WFS are listed in Table 5.

Table 5. High order LGS WFS main parameters

Parameter	Value
FoV	5 arcsec diameter
n. of sub-apertures	40×40
Pixels per sub-aperture per pupil	6×6
Pixel scale	0.83 arcsec/pixel
Pupil size	5.760 mm
Lenslet pitch	0.144 mm
Lenlset focal length	4.217 mm
Detector	CCD220
Maximum frame rate	1200 Hz

4.6 WFS cameras

The WFS sensor cameras consists of the CCD220 package attached to the ESO front end electronics, in its mechanical housing. The CCD220 package is made of the mechanical package itself, housing the focal plane array and sealed by a Sapphire window. The CCD220 is an Electron Multiplying CCD detector (EMCCD) where the accumulated charge created by the incident photons is amplified by the impact ionization during the transfer across several stages of a

dedicated register. When the amplified charge is read-out the associated noise (RON), which is not amplified, becomes negligible with respect the signal. EMCCD allows equivalent RON much smaller than 1e-/px/frame. The main characteristics of the CCD220 are listed in Table 6.

Table 6. CCD220 main characteristics

Parameter	Value	Note
Image area	5.76 × 5.76 mm	-
Image section active pixels	240 (H) × 240 (V)	-
Image pixel size	24 × 24 μm	-
Additional transition rows	2	-
Number of output amplifiers	8	-
Fill factor	100%	-
Peak charge storage (image area)	300 ke$^-$/px	@ gain =1
Dark signal	1.0 e$^-$/px/s	Average on meas. on 18 chips
RON (gain 1)	90 e$^-$/px/frame	Average on meas. on 18 chips
Max multiplication register gain	1000	-
Excess noise factor	$\sqrt{2}$	-

5. REAL-TIME COMPUTER DESIGN

The ERIS Real-Time Computer (RTC) is based on ESOs Standard Platform for Adaptive Optics Real-Time Applications (SPARTA). At the time of writing (June 2012), SPARTA systems are already being used by three VLT 2nd generation instruments. The RTC for SPHERE is finalized and has been tested with SAXO in the lab including closure of all AO loops. The RTCs for the other two AOF AO systems GRAAL and GALACSI are currently under development.

5.1 Overview

The SPARTA RTC consists of two main building blocks:

- The RTC box: a 19” VXS chassis hosting a number of dedicated computing boards. The hard real-time AO loops are handled by this unit. All sensors and actuators are connected here
- The Co-processing cluster: a number of Linux servers which receive real-time data from the RTC box and handle all soft real-time functionalities like calibration, optimization, data recording, measurements and performance estimation

Both building blocks are interconnected through a dedicated private network.

The sensors and actuators connected to SPARTA are:

- LGS SHWFS: 240x240 pixels, 40x40 sub-apertures, 6x6 pixels per sub-aperture, max. frame rate 1200Hz, 1240 valid sub-apertures. This is the same sensor as already used with SPHERE. It has already been tested with SPARTA.
- NGS PWFS: configuration depending on mode. Most demanding configuration is: 240x240 pixels, 40x40 sub-apertures. Max. frame rate 1200Hz, 1256 valid sub-apertures. The IF between NGC and SPARTA is the same as for the LGS WFS.
- DSM: 1170 actuators
- 4LGSF jitter actuators: 4 fast and 4 slow tip/tilt actuators

Note that the fast tip/tilt actuator for modulation in front of the PWFS and the pupil centering mirrors are not controlled by SPARTA.

The SPARTA system for ERIS will heavily re-use what has been developed for the existing systems. A schematic view of the SPARTA system is given in Figure 8.

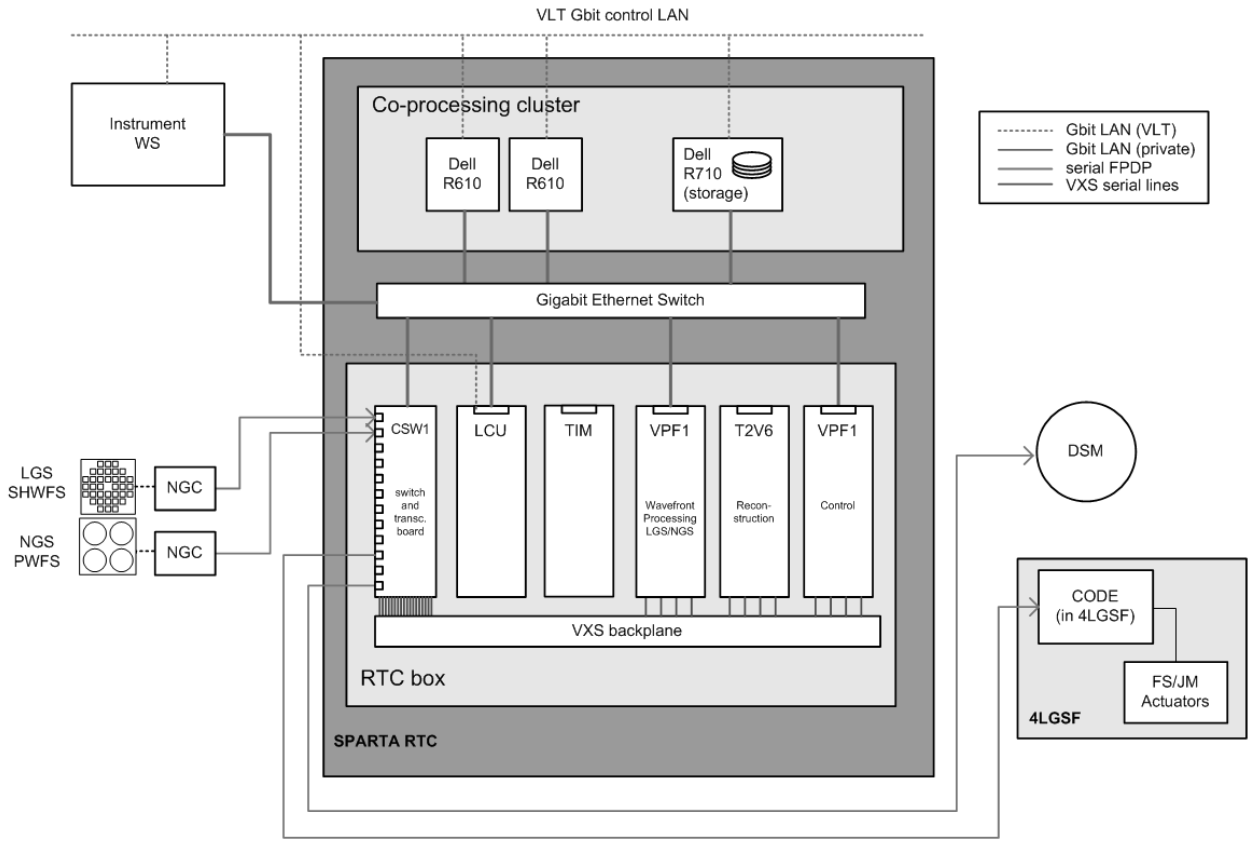

Figure 8. SPARTA system

5.2 Hardware design

The ERIS RTC box uses 3 processing boards:

- VPF1 acquisition: this board hosts the two WPUs for the SH WFS and the PWFS. In NGS mode, only the PWFS is used.
- T2V6 reconstruction: this board handles the projection of slopes into mirror space for the HO sensor (depending on mode LGS/NGS). In case on-the-fly matrix swapping with frame losses below 10 frames should be required, a second T2V6 board has to be added.
- VPF1 control: the operations on this board depend on the mode:
- NGS: delta positions are received from the T2V6 board and the IIR filter is applied. Mirror commands are sent to the DSM
- LGS: same as NGS but in addition, also the slopes from the LO NGS sensor are received, projected into DSM space, passed through an IIR filter and added to the control vector.

Data routing inside the RTC box and external fiber interfaces are handled by the CSW1 board.

The co-processing cluster will be made of the following components:

- 1 Dell PowerEdge R710 server: this is the machine known as the concentrator. It receives all real-time data from the RTC box, re-distributes it to the other cluster servers and is capable of recording real-time data on its internal RAID storage array.
- 2 Dell PowerEdge R610 servers: these machines handle processing tasks like calibration, optimization, statistics, etc…
- The RTC-box and the co-processing cluster will be interconnected via dedicated private networks. Therefore every host is connected to a CISCO 3750X switch.
- In addition, there will be a terminal server for access to the serial ports of all RTC box boards and a monitoring system for temperatures, voltages and fan status of the RTC box.

5.3 Software design

The SW architecture of the ERIS RTC is the same as for all other SPARTA systems. The difference is in the number and type of objects running in the co-processing cluster and their configuration.

Those objects providing general services like data distribution, recording, configuration management, disturbance injection and others exist – they are provided with the SPARTA common software. A number of objects already implemented for SPHERE, GRAAL or GALACSI can be reused – possibly with small adaptations. Examples would be the atmospheric statistics, performance estimation or the WFS optimization (dark following, flat measurement, etc…).

Certain objects which handle functionality specific to ERIS will have to be developed. These will mainly be related to the PWFS.

5.4 Performance estimation

The systems dimensions of the ERIS RTC are partly comparable to the ones of SPHERE (1240 sub-apertures, 1377 actuators, 1200Hz frame rate). Therefore, the following performance can be expected based on previous experience:

- LGS mode: 70µs from last pixel received to first command sent out (pure RTC delay)
- NGS mode: approx. 140 µs (due to the PWFS readout) from last pixel received to first command sent out (pure RTC delay)

6. CONCLUSIONS

The design of the ERIS AO module has been presented. The AO design has been derived from the instrument TLRs.

Detailed numerical simulations have been carried out to evaluate the system performance for its observing modes (NGS and LGS). The PWFS has been chosen as baseline for NGS WFS (high and low order) the advantage vs. classical SHWFS is on the significantly higher correction performance and the combination of high and low order allowing to reduce the number of WFSs on board.

The optical design has been presented for both NGS and LGS paths. It has been proven that such AO architecture can fit in the reduced volume available at VLT Cassegrain focus. ERIS will benefit from AOF developments, namely DSM, 4LGSF and ancillary sub-systems such as SPARTA RTC, CCD220 WFS cameras and ESO controllers. In the specific the SPARTA design can, as of today, comfortably control the ERIS AO module with minor modifications related to PWFS implementation.

ERIS will deliver the highest ever achieved by any AO system in NGS mode, and will be extremely competitive in LGS mode especially for the sky coverage. The ERIS project just completed the Phase A study and is awaiting for approval to continue to the next phases.

REFERENCES

[1] Amico, P., Marchetti, E., Baruffolo, A., Delabre, B., Duchateau, M., Ekinci, M., Fantinel, D., Finger, G., Frank, C., Hofmann, R., Jolley, P., Lizon, J.-L., Weisz, H., “Design of ERIS for the VLT,” Proc. SPIE 8446, 8446-71 (2012).

[2] Arsenault, R., Madec, P.-Y., Hubin, N., Stroebele, S., Paufique, J., Vernet, E., Hackenberg, W. K. P., Pirard, J., Jochum, L., Glindemann, A., Jost, A., Conzelmann, R. D., Kiekebusch, M. J., Tordo, S., Lizon, J.-L., Donaldson, R., Fedrigo, E., Soenke, C., Duchateau, M., Bruton, A., Delabre, B., Downing, M. D., Reyes Moreno, J., Kolb, J., Bechet, C., Le Louarn, M., Manescau, A., Bonaccini Calia, D., Quattri, M., Guidolin, I. M., Buzzoni, B., Dupuy, C., Guzman, R., Comin, M., Silber, A., Quentin, J., Jolley, P., Heinz, V., Argomedo, J., Gallieni, D., Lazzarini, P. G., Biasi, R., Andrighettoni, M., Angerer, G., Pescoller, D., La Penna, P., Stuik, R., Deep, A., "Manufacturing of the ESO adaptive optics Facility ," Proc. SPIE 7736, 77360L-77360L-11 (2010).

[3] Bonnet, H., Abuter, R., Baker, A., Bornemann, W., Brown, A., Castillo, R.., Conzelmann, R., Damster, R., Davies, R., Delabre, B., Donaldson, R., Dumas, C., Eisenhauer, F., Elswijk, E., Fedrigo, E., Finger, G., Gemperlein, H., Genzel, R., Gilbert, A., Gillet, G., Goldbrunner, A., Horribin, M., ter Horts, R., Huber, S., Hubin, N., Iserlohe, C., Kaufer, A., Kissler-Patig, M., Kragt, J., Kroes, G., Lehnert, M., Lieb, W., Liske, J., Lizon, J.-L., Lutz, D., Modigliani, A., Monnet, G., Nesvabda, N., Patig, J., Pragt, J., Reunanen, J., Röhrle C., Rossi, S., Schmutzer, R., Schoenmaker, T., Schreiber, J., Ströbele, S., Szeifert, T., Tacconi, L., Tecza, M., Thatte, N., Tordo, S., van der Werf, P., Weisz, H., “First Light of SINFONI at the VLT,” Messenger 117, 17-24 (2004).

[4] Brandner, W., Rousset, G., Lenzen, R., Hubin, N., Lacombe, F., Hofmann, R., Moorwood, A., Lagrange, A.-M., Gendron, E., Hartung, M., Puget, P., Ageorges, N., Biereichel, P., Bouy, H., Charton, J., Dumont, G., Fusco, T., Jung, Y., Lehnert, M., Liozn, J.-L., Monnet, G., Mouillet, D., Moutou, C., Rabaud, D., Röhrle, C., Skole, S., Spyromilio, J., Storz, C., Tacconi-Garman, L., Zins, G., “NAOS+CONICA at YEPUN: First VLT Adaptive Optics System Sees First Light,” Messenger 107, 1-6 (2002).

[5] Fedrigo, E., Donaldson, R., Suarez Valles, M., Soenke, C., Zampieri, S., Bourtembourg, R., "SPARTA for the VLT: status and plans," Proc. SPIE 7736, 77362I-77362I-10 (2010).

[6] Le Louarn, M., Verinaud, C., Korkiakoski, V., Fedrigo, E., “Parallel simulation tools for AO on ELTs,” Proc. SPIE 5490, 705-712 (2004).